

**Author accepted manuscript document released under the terms of a
Creative Commons CC-BY licence using the
Swansea University Research Publications Policy**

<https://creativecommons.org/licenses/by/4.0/>

1 Evaluation of Lead Shielding Against Head Leakage from a
2 6 MV Agility Linac Using FLUKA Monte Carlo Simulation

3 Turki Almatani^{1,*} and Richard P. Hugtenburg^{2,3}

4 ¹*Umm Al-Qura University, Makkah, KSA*

5 ²*College of Medicine, Swansea University, Singleton Park, Swansea SA2 8PP, UK*

6 ³*Department of Medical Physics and Clinical Engineering, Swansea Bay University Health Board,*
7 *Swansea SA2 8QA, UK*

*Corresponding author. E-mail address: tumatani@uqu.edu.sa (T. Almatani)

Most studies in the literature focus on in-field dosimetry, with relatively few addressing the accuracy of linear accelerator (linac) models in leakage or out-of-field regions. This study investigates leakage radiation from a linac using Monte Carlo (MC) simulations. An Elekta Synergy linac equipped with an Agility head was modelled using the FLUKA code. Head leakage radiation measurements were performed using a 6 MV photon beam directed both horizontally and vertically. A PTW Spherical Chamber (TK-30) was used to acquire measurements at 13 different locations, each at a fixed source-to-chamber distance of 100 cm. The ion chamber was also explicitly modelled in the simulations. Based on the mean photon energy at each position, the required lead shielding thickness was initially calculated using narrow-beam linear attenuation coefficients. To account for broad-beam geometry, buildup factors—dependent on photon energy and the number of mean free paths—were incorporated. An iterative method was applied until the calculated shielding thicknesses converged. All measured leakage values were within the recommended limit of 0.1% of the maximum absorbed dose at the isocentre, ranging from 0.01% to 0.06%, except at the isocentre itself, which exceeded the limit. The MC simulation results showed good agreement with the measurements. The calculated lead thicknesses required to match the measured leakage ranged from 3.6 cm to 13 cm, depending on the location. This would help improve shielding accuracy and reduce secondary cancer risk from leakage or out-of-field exposure.

28

KEYWORDS: Leakage; Agility head; Monte Carlo ; FLUKA.

29

1. Introduction

The measurement of linear accelerator (linac) head leakage radiation is a crucial aspect of acceptance testing during commissioning to ensure the safety of both patients and staff (Jaradat and Biggs, 2007). In clinical settings, radiation from a linac includes the intended primary beam, as well as scattered and unintended leakage radiation. Leakage radiation refers to the portion of radiation that escapes through the shielded head of the linac in all directions when the beam is on. It differs from primary or scattered radiation, as it does not contribute to the therapeutic dose but can lead to unnecessary exposure in surrounding areas. Regulations, such as those outlined in National Council on Radiation Protection and Measurements (NCRP) Report 49, generally mandate that shielding must limit leakage radiation to no more than 0.1% of the primary beam's exposure at a distance of 1 meter from the source (NCRP, 1976; ICRP, 1991). However, leakage radiation is not uniformly distributed in all directions. The magnitude of leakage radiation depends on several factors, including measurement position, gantry angle, beam energy, and beam current or power (Jaradat and Biggs, 2007).

The extent of leakage radiation primarily depends on the shielding effectiveness of the treatment head's wall, making it essential to verify the adequacy of this shielding during commissioning. Leakage radiation assessments typically involve measurements at different positions around the linac head, including forward, lateral, and backward directions. Several studies have investigated and measured head leakage for various linac models using different detectors (Kase et al., 1983; McParland and Fair, 1992; Van der Giessen, 1994; Stern 1999; Jaradat and Biggs, 2007; Lonski et al., 2012; Attalla, 2013; Kinsara et al., 2016; Al-Saleh and Hugtenburg, 2023; Benazon et al., 2023).

Although head scatter and leakage radiation levels are generally low, prolonged exposure may contribute to unwanted radiation doses to both patients and staff (ICRP, 1991; Kinsara et al., 2016). For radiotherapy staff, chronic low-level exposure, particu-

larly during frequent or prolonged procedures near the linac, can accumulate over time, potentially increasing the long-term risk of stochastic effects such as secondary cancers. In clinical practice, minimizing unnecessary exposure aligns with the ALARA (As Low As Reasonably Achievable) principle (ICRP, 1991). This underscores the need for precise modelling and measurement of linac head leakage, not only for regulatory compliance, but also to protect healthcare workers and ensure long-term treatment quality and safety.

Given the importance of accurately assessing leakage radiation for both regulatory compliance and patient safety, various analytical and modelling approaches have been used to improve measurement precision (Al-Saleh and Hugtenburg, 2023; Benazon et al., 2023). Among these, Monte Carlo (MC) simulation of linac heads has long been a standard approach for investigating various dosimetric properties. While most studies in the literature focus on in-field dosimetry using different linacs, relatively few have examined the accuracy of linac head models in leakage or out-of-field regions (Nelson and LaRiviere, 1984; Molazadeh et al., 2017; Ghasemi-Jangjoo and Ghiasi, 2020; Al-Saleh and Hugtenburg, 2023). For the Elekta linac with an Agility head, a few studies have investigated multi-leaf collimator (MLC) leakage and in-field dosimetry using different energies (Gholampourkashi et al., 2018; Ohira et al., 2020; Almatani et al., 2022; Al-Saleh and Hugtenburg, 2023; Jacquet et al., 2024).

This study aims to investigate and quantify head scatter and leakage radiation from the Elekta linac Agility head at various angles and distances. Additionally, it seeks to evaluate the head shielding thickness using FLUKA MC simulations by comparing the simulated results with experimental measurements.

2. Method and materials

2.1. *Equipment and Measurement Setup*

This study utilized the 6 MV photon beam from the Elekta Synergy linac with an Agility head at Singleton Hospital, Swansea, UK (ElektaTM, UK). The linac is capable of producing two beam energies: 6 MV and 10 MV. For the 10 MV photon beam, the primary collimator rotates from an open port to a filtered port, functioning both as a primary collimator and an additional flattening filter, which adds complexity to accurate simulation (Almatani et al., 2022). Although this study focuses on the 6 MV photon beam, both the open and filtered port configurations of the primary collimator were modelled (see Section 2.2).

For head scatter and leakage measurements, a TK-30 spherical ionization chamber with a sensitive volume of 27.9 cm³, manufactured by PTW-Freiburg (PTW, Germany), was used. The chamber's energy response remains within $\leq \pm 5\%$ across the energy range from 48 keV to ⁶⁰Co. The chamber had a radius of 1.88 cm, and its sensitive wall volume is composed of 3 mm of POM (Polyoxymethylene), 0.02 mm of graphite, and 0.22 mm of lacquer.

2.2. *FLUKA MC model*

The treatment head components of the Elekta linac with the Agility head were modelled using the FLUKA MC code (Fasso et al., 2005; Böhlen et al., 2014). Flair was used to generate and edit the input cards, visualize the geometry, and process the output files (Vlachoudis, 2009). The model includes the target and copper support, the primary collimator in both open and filtered port configurations, the flattening filter, the ion chamber, the MLC, and the jaws, as shown in Figure 1. The tungsten density and composition of the MLC and jaws were set to 18.0 g/cm³, comprising 95% tungsten, 3.75% nickel, and 1.25% iron, in accordance with the vendor's specifications (Ohira at

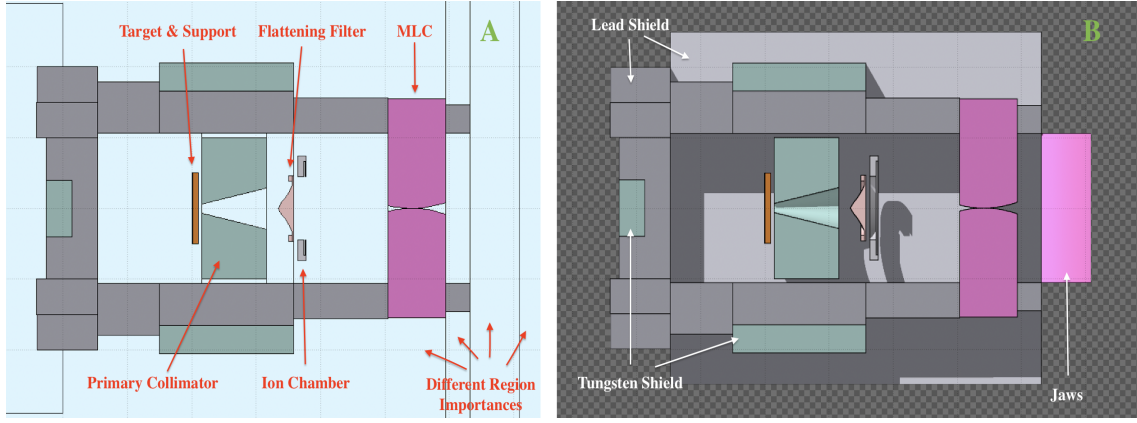


Figure 1: FLUKA linac model components and shields: (A) 2D view and (B) 3D view.

al., 2020)).

The electron beam energy incident on the target was set to 6.1 MeV. The beam had a Gaussian spatial distribution with a full width at half maximum (FWHM) of 0.14 cm in both the x and y directions. The beam was centred at the origin (0, 0, 0) in x, y, and z coordinates, and its direction was aligned along the positive z-axis.

The radiation source and linac components are located within a region called "void," which is surrounded by a "black hole" region where all particles are fully absorbed and vanished. The void is subdivided into regions with varying importances as part of a biasing technique to optimize computing efficiency (Böhlen et al., 2014). To avoid correlated tallies, the importances were continuously and gradually increased from the target to the region of interest. The importance biasing ratio between regions was 10. Additionally, the energy cutoffs for electron transport and production were set to 189 keV, while those for photon transport and production were set to 10 keV.

Prior to performing the leakage simulations, the FLUKA MC model was validated and adjusted based on measured data. This validation included a comparison of the percentage depth dose (PDD) curve for a $10 \times 10 \text{ cm}^2$ field size at a 90 cm source-to-surface distance (SSD), as well as the beam quality index, with experimental measurements. To calculate the quality index, the dose at a depth of 20 cm was divided by the dose at a depth of 10 cm. Although different SSDs were used, the total distance from the source to the scoring chamber was consistently maintained at 100 cm.

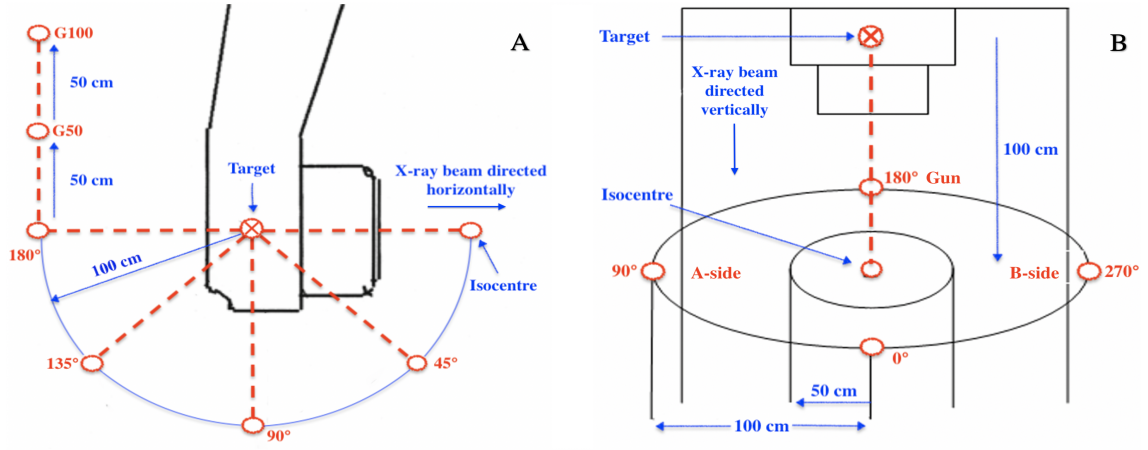


Figure 2: Measurement locations for (A) horizontal and (B) vertical beam directions.

2.3. Leakage measurement

The head leakage radiation measurements were performed with the 6 MV photon beam directed both horizontally and vertically, as shown in Figure 2. In both configurations, the jaws were fully closed, while the MLC was opened to $0.5 \times 0.5 \text{ cm}^2$.

For horizontal irradiation, leakage measurements were taken at angles of 180° , 135° , 90° , and 45° along a circular path with a radius of 100 cm, centred at the isocenter. Additionally, two measurements were conducted at 50 cm (G50) and 100 cm (G100) vertically above the 180° position.

For vertical irradiation (where the beam is directed downward toward the patient plane), measurements were taken at angles of 0° , 90° , 180° , and 270° along two circular paths with radii of 50 cm and 100 cm, centred at the isocentre. All measurements were then normalized and expressed as a percentage relative to a reference dose at the isocentre, measured at a 100 cm source-to-axis distance (SAD) with a $10 \times 10 \text{ cm}^2$ field size. This would eliminate the influence of beam current.

2.4. Leakage simulation and shield thickness calculation

The TK-30 spherical ionization chamber was modelled in the FLUKA simulation. The chamber water-equivalent sensitive wall thickness was 0.78 cm. Then the chamber model was placed at each of the measurement locations mentioned above using the same setup.

For each chamber position, the USRBIN card was used with "dose" as scoring quantity with "region point" type, where the statistical convergence is much faster and more accurate than "region" type (Böhlen et al., 2014). The dose was scored in units of $\text{GeV}\cdot\text{cm}^3/\text{g}$ per particle, which corresponds to the energy deposited divided by the air density. To convert this to dose in Gy per particle, the scored value was multiplied by the chamber volume and by the conversion factor from electron volts to joules. Similar to the measurements, all simulation results were normalized and expressed as a percentage relative to a reference dose at the isocentre, measured at a SAD 100 cm with a 10×10 cm^2 field size.

In addition, the USRTRACK card was used at each chamber position to obtain the track-length density distribution, normalized to the chamber volume. The fluence energy spectrum was then calculated by multiplying each energy bin by its width, followed by determining the mean energy at each location. Consequently, by comparing the results with measurements and assuming a narrow-beam geometry, the initial lead thickness required to reduce leakage in each direction was estimated. To account for broad-beam geometry, buildup (B) factors were then incorporated, depending on photon energy and the number of mean free paths in the absorber (Shleien, 1992). Through iterative calculations, the required lead shield thickness for each location was determined. An additional complexity was that some parts of the lead shield were embedded with tungsten blocks, as observed from the linac after removing the cover as shown in Figure 3.

3. Results

The FLUKA Monte Carlo simulations were performed using two systems: a Linux Ubuntu PC with a 3.4 GHz 16-core CPU and 32 GB RAM, and an iMac Pro with a 2.3 GHz 18-core Intel Xeon W processor and 128 GB RAM. Different random number seeds were used to generate independent input files on each system. Using the 'Spawn' option in Flair, 16 input files were generated on the Linux system and 18 on the iMac



Figure 3: Linac head with the cover removed.

Pro, all executed in parallel with unique seeds to minimize statistical uncertainty. A total of 800 million particle histories were simulated on each system, and the results were combined for analysis.

Figure 4 shows the PDD curves and relative difference curve of the MC model and the measured data. The maximum deviation, approximately -7% , was observed in the build-up region. Overall, the MC model shows good agreement with measurements, with a mean difference of -1.2% . Additionally, the measured quality index was 0.679, while the simulated value was 0.672, resulting in a -1% difference.

Table 1 presents the leakage measurement results for different positions with the beam directed horizontally. To enhance measurement accuracy, 200 monitor unit (MU) was delivered for each leakage measurement, allowing the ion chamber to collect more charge, thereby improving the signal and reducing statistical uncertainty. The measured values were then divided by 10 before normalization to the reference dose for a delivered 20 MU, with the output calibrated to 1 cGy/MU.

Figure 5 illustrates the MC model for leakage measurement with the beam directed

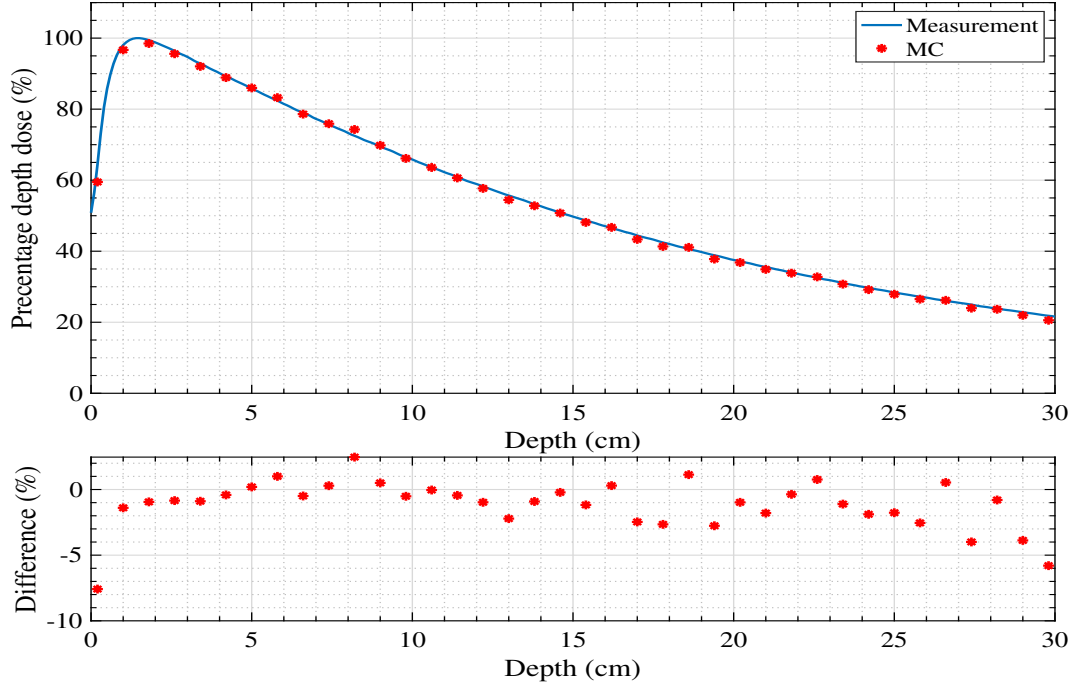


Figure 4: Comparison of PDD curve between MC and measurement.

horizontally, highlighting different region importance biasing. The corresponding MC simulation results are presented in Table 1. The highest leakage measurement was observed at the isocentre and then at the 180° position (backscatter), while the lowest—accompanied by the highest uncertainty—was recorded at the 45° position. However, the calculated lead shield thickness required to match the measured leakage was approximately 8.4 cm at the 180° position and 13.6 cm at the 90° position, both embedded with 4 cm tungsten blocks. At the 135° and 45° positions, the required lead shield

Table 1: Leakage measurement positions when the beam is directed horizontally.

Chamber position	Leakage (%)		MC statistical uncertainty (%)
	Measurement	MC simulation	
G100	0.03	0.023	16
G50	0.05	0.047	13
180°	0.06	0.068	10
135°	0.05	0.045	14
90°	0.02	0.036	11
45°	0.01	0.016	20
Isocentre	0.547	0.576	6

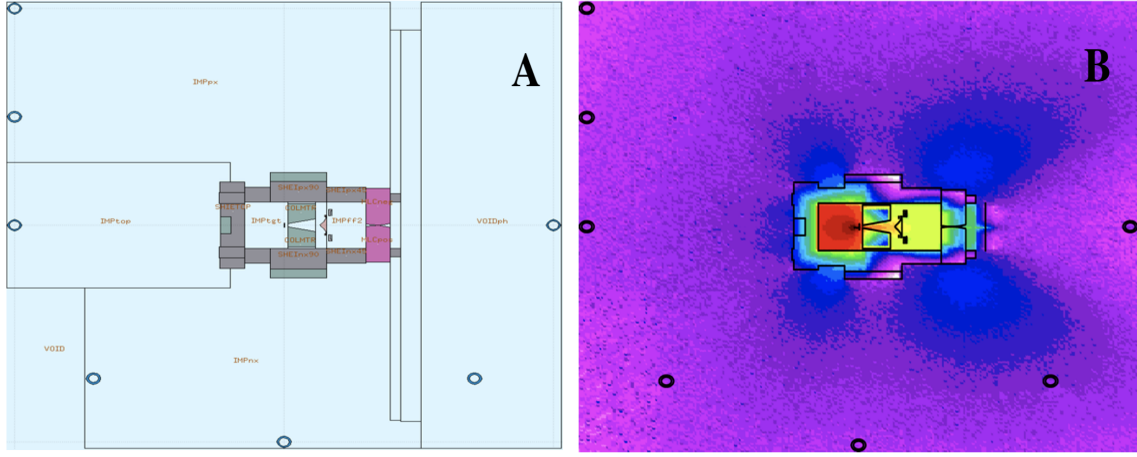


Figure 5: (A) FLUKA simulation geometry with different chamber locations; (B) same geometry with overlaid dose distribution.

189 thickness was around 7 cm and 6.8 cm, respectively. For the G50 and G100 positions,
 190 the estimated lead shield thickness was 9.5 cm and 9.2 cm, respectively.

191 Table 2 presents the leakage measurement results for various positions with the beam
 192 directed vertically, corresponding to the patient plane. The same MU technique used for
 193 the horizontal irradiation (Table 1) was applied. The highest leakage measurement was
 194 observed at the 180° (Gun) position, while the lowest was recorded at the 0° position.

195 In general, the MC simulation results were in good agreement with the measure-
 196 ments. The calculated lead shield thickness required to match the measured leakage
 197 was approximately 4.8 cm at the 0° position and 3.6 cm at 180°. At the 90° and 270°

Table 2: Leakage measurement positions when the beam is directed vertically.

Chamber position	Radius	Leakage (%)		MC statistical uncertainty (%)
		Measurement	Simulation	
90° (A-side)	50 cm	0.02	0.025	14
90° (A-side)	100 cm	0.02	0.008	18
0°	50 cm	0.01	0.013	22
0°	100 cm	0.01	0.024	23
270° (B-side)	50 cm	0.02	0.021	19
270° (B-side)	100 cm	0.02	0.006	30
180° (Gun)	50 cm	0.03	0.021	18

198 positions, the estimated lead thickness was around 4 cm.

199 4. Discussion

200 The comparison between the simulated and measured PDD curves (Figure 4) demon-
201 strates the overall accuracy of the FLUKA MC model. The MC model generally shows
202 good agreement with the measured data, with a mean difference of -1.2% . Therefore,
203 the simulation results demonstrated generally good agreement with the measured leak-
204 age doses across most angles and distances. However, some discrepancies were observed.
205 These differences may be partly due to the fact that the ion chamber does not have a
206 uniform response outside the 48 keV to ^{60}Co energy range. These variations in leakage
207 radiation levels are influenced not only by differences in the effective shielding thick-
208 ness of the head wall but also by variations in the distances between the target and
209 measurement locations. Additionally, experimental uncertainties in dosimetric measure-
210 ments—such as slight variations in ion chamber positioning, environmental factors, and
211 statistical fluctuations—may further contribute to these discrepancies. The detector has
212 a range of validity where the uncertainty lies within 5%. Outside of this range, such as
213 in the primary beam, the uncertainty can be greater. The detector’s leakage current is
214 $\leq \pm 5$ fA. Other sources of uncertainty, such as measurement reproducibility and dose
215 linearity, are assumed to be negligible.

216 For MC simulation, the lead thicknesses were calculated using B factors based on
217 the mean energy scored at each position. In general, the B factor is defined as the
218 ratio of total radiation (including primary, scattered, and secondary components) to
219 primary radiation alone. For a broad-beam geometry, the B factor is always greater
220 than 1. However, it depends on several factors, including photon energy, the thickness
221 and attenuating medium, and the geometric conditions. As a result, the effective linear
222 attenuation coefficient (μ') is lower than the linear attenuation coefficient (μ). Instead
223 of using B factors, energy-absorption coefficients are sometimes used as an approxima-

tion, though this is generally considered a poor substitute (Attix, 2008). However, a key challenge in using B factors is that they depend on the product of thickness and the linear attenuation coefficient (μ) (expressed as the number of mean free paths), while the thickness itself is the parameter being determined. To resolve this, an iterative approach is applied until convergence is reached. First, the required thickness is estimated assuming a narrow-beam geometry. Then, the corresponding B factor for this thickness is used to update the thickness calculation. This process is repeated, with each newly calculated thickness being used to determine an updated B factor, until the thickness value stabilizes and no longer changes.

The highest statistical uncertainty was observed at the 270° position with a 100 cm radius, reaching up to 30%, due to the low number of photons reaching that location. Increasing the number of photon interactions at this or similar positions would require a substantial increase in simulated particle histories—and consequently, longer simulation times. In this study, 800 million histories were simulated, requiring approximately one week using 16-core and 18-core CPU systems. For future studies, this uncertainty could be reduced by either increasing the simulation time or utilizing the USRTRACK card to derive the deposited dose from photon energy fluence and mass attenuation coefficients, rather than relying on energy deposition in the detector, however this has been found to inaccurately reproduce the dose. The electron component of the linac leakage is an important and often ignored component in modelling studies. Using mass attenuation coefficients instead of mass energy absorption coefficients better accounts for the lack of charged particle equilibrium that would be required to determine the dose due to the photon component, especially when the chamber wall thickness is not sufficient to fully stop secondary electrons. Consequently, the results cannot be easily extrapolated to a greater distance or with penetration through an external barrier.

5. Conclusion

The MC model was first validated against measured PDD and quality index data, confirming its accuracy with a mean PDD difference of -1.2% and a quality index deviation of -1% . Using this validated model, the FLUKA simulations showed good agreement with the experimental leakage radiation measurements around the Elekta Synergy linac with an Agility head.

By incorporating buildup factors and iteratively calculating lead thicknesses based on mean photon energies, the model accurately predicted the shielding requirements at various positions. The calculated lead thicknesses required to match the measured leakage ranged from 3.6 cm to 13.6 cm, with the highest leakage observed at the isocentre and 180° positions, and the lowest, accompanied by the highest uncertainty, at 45° .

These findings confirm that even small variations in geometry and shielding can significantly impact leakage levels. This highlights the importance of precise Monte Carlo modelling for evaluating leakage and out-of-field dose, which is essential for improving radiation protection and minimizing the long-term risk of secondary cancers.

6. Reference

Al-Saleh, W.M., Almatani, T., 2024. A Monte Carlo model of an agility head for a 6 MV Elekta photon beam. *Radiation Physics and Chemistry* 216, 111433.

Al-Saleh, W.M., Hugtenburg, R.P., 2023. Monte Carlo modelling of a 6 MV Elekta linear accelerator for in-field and out-of-field dosimetry. *Radiation Physics and Chemistry* 203, 110584.

Almatani, T., Hugtenburg, R.P., Smakovs, A., 2022. A Monte Carlo model of an agility head for a 10-MV photon beam. *Journal of Taibah University for Science* 16 (1), 300–307.

Attalla, E.M., 2013. Comparison of two methods for assessing leakage radiation dose around the head of the medical linear accelerators. *The Chinese-German Journal of Clinical Oncology* 12, 435-438.

Attix, F.H., 2008. Introduction to radiological physics and radiation dosimetry. John Wiley & Sons.

Benzazon, N., Colnot, J., de Kermenguy, F., Achkar, S., de Vathaire, F., Deutsch, E., Robert, C., Diallo, I., 2023. Analytical models for external photon beam radiotherapy out-of-field dose calculation: a scoping review. *Front. Oncol.* 13.

Böhlen, T.T., Cerutti, F., Chin, M.P.W., Fassò, A., Ferrari, A., Ortega, P.G., Mairani, A., Sala, P.R., Smirnov, G., Vlachoudis, V., 2014. The FLUKA code: developments and challenges for high energy and medical applications. *Nuclear Data Sheets* 120, 211-214.

Fasso, A., Ferrari, A., Ranft, J., Sala, P.R., 2005. FLUKA: a multi-particle transport code (24-28). CERN-2005-10.

Ghasemi-Jangjoo, A., Ghiasi, H., 2020. Application of the phase-space distribution approach of Monte Carlo for radiation contamination dose estimation from the (n,γ) , (γ,n) nuclear reactions and linac leakage photons in the megavoltage radiotherapy facil-

ity. Reports of Practical Oncology and Radiotherapy 25 (2), 233–240.

International Commission on Radiological Protection (ICRP), 1991. ICRP Publication 60: Recommendations of the International Commission on Radiological Protection. Oxford and New York: Pergamon Press.

Jacquet, M., Baudier, T., Deutsch, E., Robert, C., Sarrut, D., 2024, July. Monte Carlo Modeling of Elekta VERSA HD for Out-of-Field Dose Characterization. In XXth International Conference on the use of Computers in Radiation therapy.

Jaradat, A.K., Biggs, P.J., 2007. Measurement of the leakage radiation from linear accelerators in the backward direction for 4, 6, 10, 15, and 18 MV X-ray energies. Health Physics 92 (4), 387–395.

Kase, K.R., Svensson, G.K., Wolbarst, A.B., Marks, M.A., 1983. Measurements of dose from secondary radiation outside a treatment field. International Journal of Radiation Oncology, Biology, Physics 9 (8), 1177–1183.

Kinsara, A., El Gizawy, A.S., Banoqitah, E., Ma, X., 2016. Review of leakage from a linear accelerator and its side effects on cancer patients. J. Nucl. Med. Radiat. Ther. 7(3), 288.

Lonski, P., Taylor, M.L., Franich, R.D., Harty, P., Kron, T., 2012. Assessment of leakage doses around the treatment heads of different linear accelerators. Radiation Protection Dosimetry 152 (4), 304–312.

McParland, B.J., Fair, H.I., 1992. A method of calculating peripheral dose distributions of photon beams below 10 MV. Medical Physics 19 (2), 283–293.

Molazadeh, M., Zeinali, A., Robatjazi, M., Shirazi, A., Geraily, G., 2017. Dosimetric characteristics of LinaTech DMLC H multi leaf collimator: Monte Carlo simulation and experimental study. J. Applied Clin. Med. Phys. 18 (2), 113–124.

Molazadeh, M., Zeinali, A., Robatjazi, M., Shirazi, A., Geraily, G., 2017. Dosimetric characteristics of LinaTech DMLC H multi leaf collimator: Monte Carlo simulation and experimental study. Journal of Applied Clinical Medical Physics 18 (2), 113–124.

317 National Council on Radiation Protection and Measurements (NCRP), 1976. NCRP
 318 Report No. 49: Structural shielding design and evaluation for megavoltage X- and
 319 gamma-ray radiotherapy facilities: Recommendations of the National Council on Radi-
 320 ation Protection and Measurements.

321 Nelson, W.R., Lariviere, P.D., 1984. Primary and Leakage Radiation Calculations
 322 at 6, 10 and 25 MeV. *Health Physics* 47 (6), 811–818.

323 Ohira, S., Takegawa, H., Miyazaki, M., Koizumi, M., Teshima, T., 2020. Monte
 324 Carlo modeling of the agility MLC for IMRT and VMAT calculations. *In Vivo* 34 (5),
 325 2371-2380.

326 Shleien, B., 1992. *The Health Physics and Radiological Health Handbook*.

327 Stern, R.L., 1999. Peripheral dose from a linear accelerator equipped with multileaf
 328 collimation. *Medical Physics* 26 (4), 559–563.

329 Taneja, S., Teruel, J.R., Hu, L., Xue, J., Barbee, D., 2020. Use of a 2-Dimensional
 330 Ionization Chamber Array to Measure Head Leakage of a Varian Truebeam® Linear Ac-
 331 celerator. *International Journal of Medical Physics, Clinical Engineering and Radiation*
 332 *Oncology* 9 (3), 87.

333 van der Giessen, P.-H., 1994. Calculation and measurement of the dose at points
 334 outside the primary beam for photon energies of 6, 10, and 23 MV. *International Journal*
 335 *of Radiation Oncology, Biology, Physics* 30 (5), 1239–1246.

336 Vlachoudis, V., 2009, May. FLAIR: a powerful but user friendly graphical interface
 337 for FLUKA. In *Proc. Int. Conf. on Mathematics, Computational Methods & Reactor*
 338 *Physics (M&C 2009)*, Saratoga Springs, New York 176, 43.